Proc. Natl. Acad. Sci. USA
Vol. 90, pp. 5209–5213, June 1993
Cell Biology

Direction of microtubule movement is an intrinsic property of the motor domains of kinesin heavy chain and *Drosophila* ncd protein

RUSSELL J. STEWART*, JOSHUA P. THALER, AND LAWRENCE S. B. GOLDSTEIN†

Department of Cellular and Developmental Biology, Harvard University, 16 Divinity Avenue, Cambridge, MA 02138

Communicated by Richard Losick, February 1, 1993 (received for review November 24, 1992)

ABSTRACT **The kinesin heavy chain and the *ncd* (non-claret disjunctional) gene product of *Drosophila* are microtubule-associated motor proteins related by sequence similarity within an ≈340-aa domain. Despite the sequence similarity, the kinesin heavy chain and ncd protein move in opposite directions on microtubules. To investigate the molecular basis for direction of movement, we created a series of truncated kinesin heavy chain and ncd proteins. We found that the conserved domain of both proteins has microtubule motor activity, although the efficiency with which ATP hydrolysis is coupled to microtubule movement declines dramatically with increasing truncation. Further, the direction of movement is intrinsic to the conserved motor domains, rather than being a consequence of domain organization or adjacent sequences.**

The microtubule cytoskeleton functions as a framework for a wide variety of intracellular movements. Many of these movements are powered by a growing number of recently discovered members of the kinesin superfamily (reviewed in refs. 1 and 2). These kinesin-like proteins are all related by sequence similarity within an ≈340-aa region. This conserved region is thought to constitute a mechanochemical motor domain, since it contains ATP- and microtubule-binding sites (3) and is contained within a larger segment of the kinesin heavy chain (KHC) previously shown to have microtubule motor activity (4). Outside of the presumed motor domain there is little sequence homology among the kinesin-like proteins. Together, these observations suggest that a modular, conserved microtubule-motor domain performs a wide variety of microtubule-based transport functions by being fused to unique tail domains that specify the cargoes. Beyond being adapted to move diverse cargoes, the motor domain of the kinesin superfamily can also move in either direction along microtubules. When expressed in *Escherichia coli* (5, 6), the ncd protein of *Drosophila*, despite ≈40% identity to the (+)-end-directed KHC within the conserved domain, moves toward the microtubule (−)-end. Conspicuously, the conserved domain of the ncd protein occurs at the C terminus (7, 8), as opposed to the N terminus of KHC and the majority of kinesin-like proteins.

The molecular organization and activities of the kinesin superfamily members raise several important questions about KHC and kinesin-like proteins. First, is the conserved domain an independent motor domain fused to inert attachment domains, or is the conserved domain a nucleotide-dependent microtubule-binding domain with sequences outside of the conserved domain contributing to or modulating motor activity? Second, how do motors with such a high degree of sequence similarity differ in the seemingly fundamental property of direction of movement along microtubules? The answers to these questions could provide important insights into the general mechanism by which kinesin-like proteins transduce chemical energy into force against their microtubule substrate. The initial step toward answering the latter question is to ask whether the features that allow KHC and ncd protein to move in opposite directions are a result of their domain organization, specific sequences outside of the motor domains, or sequences within the motor domain.

To address these questions we created a series of fusion proteins with truncated KHC and ncd proteins. The resulting proteins were purified from *E. coli* and assayed for ATPase and microtubule motor activities *in vitro*. We found that the conserved domains of both KHC and ncd have motor activity, although the efficiency of the motor domains declines drastically as the proteins are increasingly truncated. Further, the direction of movement of both KHC and ncd is determined within their motor domains.

MATERIALS AND METHODS

KHC–Spectrin Plasmids. The plasmid pET-K410-sp was constructed by ligation of a 3.8-kb *Eco*RI fragment of α-spectrin cDNA clone 9A (9), which was blunted with the Klenow fragment of DNA polymerase I, into the *Eag* I site of pET-K447 (4). pET-K339-sp was constructed by ligating the α-spectrin *Eco*RI fragment into the *Hpa* I site of pET-K447. To construct pET-sp-K447, the *Nhe* I site of pET-K447 was converted into an *Eco*RI site with an *Nhe* I/*Eco*RI adapter oligodeoxynucleotide. The α-spectrin *Eco*RI fragment was then ligated into the newly created *Eco*RI site. The sp-K447 protein has the additional sequence Asp-Pro-Asn at its C terminus. pET-sp-K339 was generated by ligating a stop codon linker into the *Hpa* I site of pET-sp-K447.

pGEX-KHC Plasmids. To construct pGEX-K410, pGEX-KIN (4) was digested with *Eag* I, blunted with Klenow polymerase, and digested with *Bam*HI. The resulting fragment was ligated into the pGEX-2T vector (10) digested with *Bam*HI and *Sma* I. pGEX-K361 was constructed by synthesizing a PCR primer corresponding to the nucleotide sequence at codon 361 with a stop codon and *Eco*RI site, and a PCR primer 5′ of the KHC *Hpa* I site. The resulting PCR product was digested with *Hpa* I and *Eco*RI and then ligated into pGEX-K410 digested with *Hpa* I and *Eco*RI. The *Sma* I–*Hpa* I fragment of pGEX-Kin was ligated into the *Sma* I site of pGEX-2T to create pGEX-K339. The glutathione *S*-transferase (GST)–KHC fusion proteins GST-K339 and GST-K410 have the additional sequence Gly-Asn-Ser-Ser at their C termini.

pGEX-NCD Plasmids. To construct pGEX-N195, pBS-NCD (8) was digested with *Afl* II, partially filled in with Klenow polymerase and an incomplete nucleotide mixture to leave a 2-base overhang of TT, and then digested with *Hin*cII. The resulting fragment was ligated into *Tth*111I-digested

The publication costs of this article were defrayed in part by page charge payment. This article must therefore be hereby marked "*advertisement*" in accordance with 18 U.S.C. §1734 solely to indicate this fact.

Abbreviations: GST, glutathione *S*-transferase; KHC, kinesin heavy chain.

*Present address: Rowland Institute for Science, 100 Cambridge Parkway, Cambridge, MA 02142.
†To whom reprint requests should be addressed.

pGEX-2T, blunted with Klenow polymerase, digested with *Eco*RI, and partially filled in with Klenow polymerase and an incomplete nucleotide mixture to leave a 2-base overhang of AA at the *Eco*RI site. pGEX-N280 and pGEX-N300 were constructed by synthesizing PCR primers, with 5′ *Xma* I sites, corresponding to the nucleotide sequences at codons 280 and 300, respectively, and a PCR primer 3′ of the NCD *Nae* I site. The resulting PCR products were digested with *Xma* I and *Nae* I, then ligated into pGEX-N195 digested with *Xma* I and *Nae* I. pGEX-N320 was constructed by creating an *Eco*RI site at codon 320 in pBS-NCD by PCR. pBS-NCD was then digested with *Eco*RI, blunted with Klenow polymerase, and digested with *Xho* I. The resulting *Eco*RI–*Xho* I fragment was ligated into *Xba* I-digested pGEX-KG (11), blunted with Klenow polymerase, and digested with *Xho* I.

Purification of KHC and NCD Fusion Proteins. Partial purification of the KHC–spectrin fusion proteins K410-sp, K339-sp, sp-K447, and sp-K339, was accomplished essentially as described previously for K447-sp (4). GST fusion proteins, with the exception of GST-K360, were partially purified from *E. coli* lysates by affinity absorption to glutathione-agarose. Midlogarithmic-phase bacterial cultures were induced with 0.5 mM isopropyl β-D-thiogalactopyranoside for 2–4 hr at 22°C. Lysates were prepared by sonication of bacterial cells in 20 mM phosphate/1 mM EDTA/1 mM phenylmethanesulfonyl fluoride at pH 7.2. Cellular debris and unlysed cells were pelleted in a microcentrifuge. The lysate was adjusted to 150 mM NaCl before the addition of glutathione-agarose beads (Sigma). After 30 min on ice, the beads were collected by centrifugation and washed extensively in PEM80 (80 mM K_2Pipes/1 mM EGTA/1 mM $MgCl_2$, pH 6.9) with 1 mM dithiothreitol. Fusion proteins were eluted from the agarose beads with 10 mM glutathione/50 μM ATP/PEM80, frozen in liquid N_2 in small aliquots, and stored at −70°C. GST-K360 lysates were prepared as described above, then passed over an orange dye-column (Amicon). GST-K360 was eluted with 0.5 M KCl.

Motility Assays. Typically, 5–200 ng of KHC or ncd fusion protein in PEM80 (pH 6.9) was mixed with additional buffer and 2 mM MgATP in an ≈10-μl grease chamber on a coverslip. Microtubules assembled from phosphocellulose-purified tubulin by the addition of 10–30 μM taxol were added to a final concentration of 1–5 μg/ml. The motility activity of the fusion proteins depended on the coverslip surface in an unpredictable manner. Full-length kinesin, full-length ncd, the KHC–spectrin fusion proteins, and GST-N320 were active when adsorbed to uncleaned and untreated coverslips. GST-K410, GST-N195, GST-N280, and GST-N300 were inactive on untreated coverslips but were active when adsorbed to coverslips that were cleaned and silanized with Sigmacote (Sigma) as described (12). GST-K339 and GST-K360 were inactive on both untreated and silanized coverslips but were active when an anti-GST serum was added to the motility assay (1:100 final dilution) after the fusion protein was adsorbed to the coverslip. The anti-GST serum dramatically increased the number of bound and moving microtubules for all of the GST fusion proteins but did not affect the rate of microtubule movement. In most cases, fetal bovine serum also increased the number of bound and moving microtubules but was not as effective as the anti-GST serum.

Microtubules were observed by video-enhanced differential interference contrast microscopy. Rates of motility were estimated from video records by measuring the displacement of microtubules after time intervals sufficient to ensure accurate measurements. The motility rate was calculated by dividing the distance moved by the time interval. The number of such rate estimates averaged for each fusion protein is reported as *n* in Fig. 1. For the slowest fusion protein, GST-K339, there was no perceptible movement in real time and it was necessary to wait ≈15 min to reliably measure the movement of the microtubules. For the majority of microtubules the rate was calculated over at least two time intervals (e.g., Fig. 2). In every such case, microtubules were observed to move steadily in the same direction between measurements. The direction of microtubule movement was determined by a slight modification of the method of Hyman (13). Brightly labeled microtubule seeds were created by assembling rhodamine-labeled tubulin in PEM80 with 10% Me_2SO at 37°C for 10 min. The labeled seeds were elongated by dilution into a 1-mg/ml solution of unlabeled tubulin prewarmed to 37°C. After 15 min, the labeled microtubules were stabilized by the addition of 10 volumes of PEM80 with 20 μM taxol. Unassembled, rhodamine-labeled tubulin in the seed solution was sufficient to mark the elongated portions of microtubules more dimly than the seed segment. The microtubule (−)-end was nearer to the bright seed.

ATPase Assays. ATP hydrolysis was measured by a molybdate/malachite green colorimetric assay for P_i (14). Briefly, aliquots (5–10 μl) of an ATPase reaction mixture, containing 5–50 μg/ml of KHC or ncd protein, were quenched with 90–95 μl of ice-cold 0.3 M $HClO_4$. An equal volume of a sodium molybdate/malachite green solution in 0.7 M HCl was added. After 5–15 min at room temperature, A_{650} of 100–300 μl of the malachite green/$HClO_4$ solution was determined in a microtiter-plate reader. ATP hydrolysis rates were corrected for ATP hydrolysis in the malachite green/$HClO_4$ solution.

RESULTS AND DISCUSSION

KHC Minimal Motor Domain. Previous work showed that the N-terminal 447 aa of KHC moved microtubules in an *in vitro* motility assay when fused, at their C termini, to an artificial tail of α-spectrin (4). This fusion protein, K447-sp, moved toward microtubule (+)-ends at rates comparable to that of native kinesin (Fig. 1*a*). Since these experiments were done before the existence and dimensions of the kinesin superfamily of proteins became fully apparent, K447-sp contains ≈100 aa in addition to the 340 aa that now define the kinesin superfamily. The algorithm of Lupas *et al.* (15) suggests that these 100 aa may form a coiled-coil. Therefore, K447-sp may contain a substantial segment of the kinesin stalk. Also, aa 340–400 of KHC are more highly conserved among different species than the stalk sequences beyond aa 400 (16), which suggests that this region may be critical to KHC function. For these reasons, we further delimited the minimal motor domain of the KHC by fusing α-spectrin to the N-terminal 410 aa (K410-sp) and the N-terminal 339 aa (K339-sp) of KHC (Fig. 1*a*). Both K410-sp and K339-sp generated (+)-end-directed movement; although K410-sp moved microtubules somewhat slower, and K339-sp significantly slower, than native kinesin. Motility by K339-sp demonstrates, at least qualitatively, that KHC sequences outside of the conserved 340-aa domain are not essential for motility.

Since the ncd protein and KHC move in opposite directions, and their motor domains are at opposite ends of their primary sequence, we created ncd analogs of KHC to determine whether the position of the KHC motor domain in the primary sequence affects direction. This set of experiments also tested the possibility that K339-sp motility was due to α-spectrin fortuitously substituting for an essential component of the KHC stalk. The N-terminal α-spectrin fusion protein with 447 aa of KHC (sp-K447) exhibited (+)-end-directed microtubule motility (Fig. 1*a*). However, in contrast to K339-sp, the N-terminal α-spectrin fusion protein with 339 aa of KHC (sp-K339) did not move microtubules, although microtubules were bound to the coverslip surface in the presence of the fusion protein. In solution, the specific ATPase activity of sp-K339 in the presence of microtubules

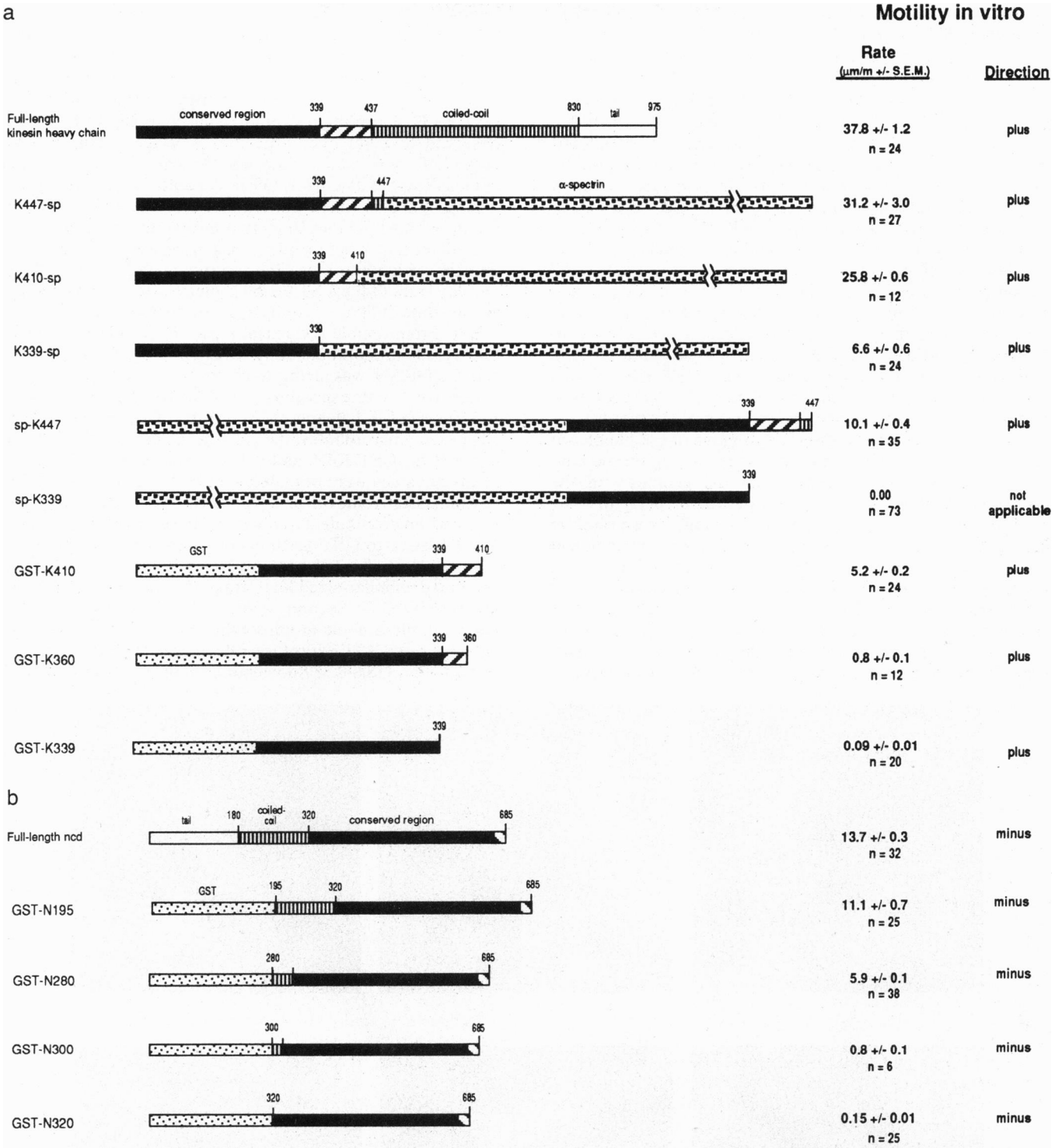

FIG. 1. Diagrams of KHC and ncd fusion proteins and summary of *in vitro* motility results. (*A*) Full-length KHC is represented in the top line with major structural features of the molecule demarcated with different shading patterns. KHC has a three-domain structure. The N terminus, containing the conserved region (black bar), forms a globular head (aa 1–340) and the central region forms an extended coiled-coil stalk (vertical stripes). The C-terminal tail is shown as an open bar. The diagonal stripes represent the region containing the SUK4 epitope. KHC fusion proteins are represented in the remaining lines. Numbers refer to KHC amino acid residues. Rates of microtubule motility and direction of movement are indicated at right; *n* is equal to the number of rate measurements (see *Materials and Methods*). Artificial tails are indicated by dotted bars (α-spectrin, larger dots; GST, smaller dots). (*B*) Full-length ncd protein is represented in the top line with the predicted three-domain structure demarcated with different shading patterns. The C terminus forms a globular domain, containing the conserved region (black bar), that is separated from the N-terminal tail structure (open bar) by a short stretch of predicted coiled-coil (vertical stripes). The C terminus of NCD extends ≈20 aa (diagonal stripes) beyond the region shared with the KHC chain. GST–ncd fusion proteins are represented in the remaining lines. Numbers refer to ncd amino acid residues.

(0.3 mg/ml) was 1.2 μmol·min^{-1}·mg^{-1}, which is comparable to or higher than native kinesin (17, 18). This suggested that the lack of motility was due to the inappropriate adsorption of the motor domain to the coverslip. Therefore, we tried GST as an alternative N-terminal artificial tail, which also allowed rapid affinity purification of the fusion proteins. The

GST fusion proteins with the N-terminal 410, 361, and 339 aa of KHC (GST-K410, GST-K361, and GST-K339) exhibited (+)-end-directed microtubule motor activity (Fig. 1*A*; (+)-end-directed microtubule motility by GST-K339 is shown in Fig. 2*a–c*). Motility by these N-terminal fusion proteins demonstrates that (+)-end-directed force can be transmitted effectively through either the N or the C terminus of the KHC motor domain, and therefore, simply reversing the orientation of the motor domain in the primary sequence does not affect direction. Furthermore, motility by GST-K339 demonstrates that the conserved region of KHC is an independent motor domain with intrinsic (+)-end directionality.

The rates of microtubule movement by the GST–KHC fusion proteins declined dramatically with increasing truncation. Microtubule motility by full-length KHC was ≈400-fold faster than that by GST-K339. Motility rates *in vitro*, though, are difficult to interpret. For example, addition of an anti-GST serum to motility assays with GST–KHC fusion proteins (see *Materials and Methods*) caused microtubule bundling. In a few instances during GST-K339 motility assays, microtubules were observed to move out of bundles at rates 4 times greater than microtubules moving on the coverslip surface, which suggests that the geometry of the coverslip motility assay can contribute, in part, to slow motility rates. That the microtubule movements we observe are due to motor activity as opposed to an ATP-independent diffusional process is evident from two observations. First, the majority of moving microtubules were observed over at least two, and often more than two, time intervals (see *Materials and Methods*). In every such case, the microtubules moved steadily in the same direction over successive time intervals; no microtubules were observed to move in opposite directions between successive time intervals. A diffusional process could not generate unidirectional movement for the number of microtubules we observed, since on time average a diffusional process would produce no net movement. Second, in a few instances during assays with GST-K339, microtubules bound to the coverslip surface were observed to bend over time into S shapes with multiple curves of short radius (data not shown). This observation demonstrates that GST-K339 is capable of generating and maintaining over time a unidirectional force, which is inconsistent with an ATP-independent diffusional process.

To determine whether misfolding or instability of the motor domain, or inhibition by GST, also contributed to the slow motility rates of the GST fusion proteins, we investigated the steady-state ATPase activities of the fusion proteins in solution. From double reciprocal plots of the ATP hydrolysis rate versus microtubule concentration, V_{max} for GST-K410 and GST-K339 was determined to be 1.7 s^{-1} and 24 s^{-1}, respectively. Correspondingly, the microtubule K_m was 1.9 μM for GST-K410 and 0.14 μM for GST-K339. In the absence of microtubules, the ATPase specific activities were 0.01 s^{-1} for GST-K410 and 0.03 s^{-1} for GST-K339. Nearly identical values were obtained with both the K410 and K339 portions after removal of GST by thrombin digestion. The elevated microtubule-activated ATPase activity of GST-K339 relative to GST-K410 is consistent with two previous reports. First, limited proteolysis of bovine brain kinesin generated a similar-sized KHC fragment with enhanced ATPase activity (17). Second, a monoclonal antibody, SUK4, inhibited microtubule motility while increasing the microtubule-activated ATP hydrolysis rate of sea urchin kinesin (18). Intriguingly, GST-K339 does not contain the SUK4 epitope

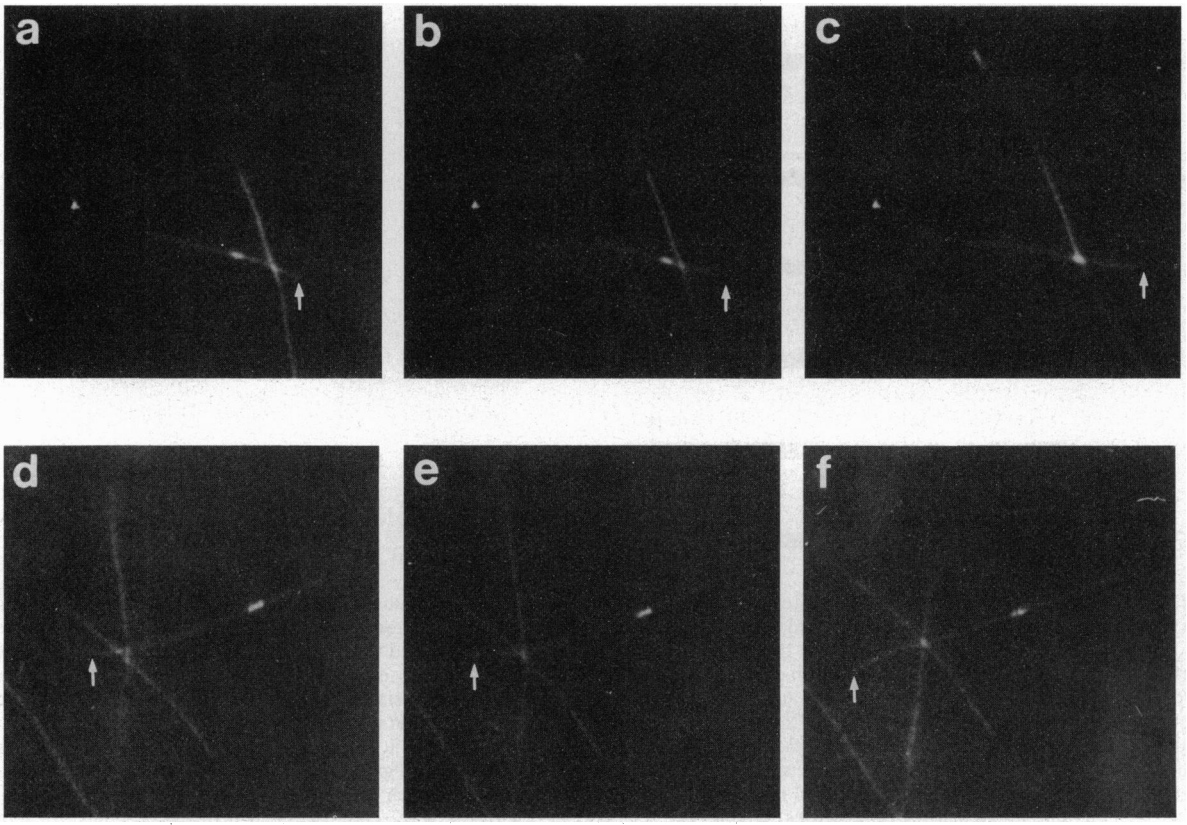

FIG. 2. Movement of polarity-marked microtubules. The microtubule (−)-end is nearer to the bright rhodamine-labeled seed because of the slower growth rate of the microtubule (−)-end during seed elongation. (*a–c*) Microtubule movements by GST-K339 during 15-min intervals. GST-K339 motility is (+)-end-directed since the microtubule (−)-end (arrows) leads (7 microtubules observed). (*d–f*) Microtubule movements by GST-N320 during 5-min intervals. The microtubule (+)-end leads (arrows), indicating that GST-N320 is (−)-end-directed (8 microtubules observed).

(data not shown). Therefore, the effect of deleting the SUK4 epitope seems to be similar to the effect of the SUK4 antibody on KHC activity.

The robust microtubule-activated ATPase activities of GST-K410 and GST-K339 suggest that the low microtubule motility rates of the truncated fusion proteins are not a result of decreased enzymatic activity. Rather, it appears that the efficiency with which ATP hydrolysis is coupled to microtubule movement decreases drastically with increasing truncation of KHC. For GST-K339, the low coupling efficiency of ATP hydrolysis and translocation may result in an increase in the apparent microtubule affinity, with a corresponding increase in the ATPase rate. More sophisticated analyses will be necessary to determine why the microtubule-activated ATPase rate of K339 is elevated. One possibility, though, in general terms, is that kinesin is conformationally biased to step toward the microtubule (+)-end after release from a tight-binding state of the mechanochemical cycle. Steady-state microtubule-activated ATP hydrolysis may then be limited by the rate that kinesin interacts with adjacent microtubule subunits. In the case of K339, truncation may have lowered the probability of a step during each ATP hydrolysis cycle, resulting in the repeated interaction of K339 with the same microtubule subunit and a consequent elevation of the microtubule-activated ATPase rate. Alternatively, as a result of truncation, K339 may step in random directions on an unobservable length scale. A slight bias of the steps toward the microtubule (+)-end could appear as slow, (+)-end-directed movement on observable length and time scales. Random instead of directed steps could alter the rate-limiting step of the ATP hydrolysis reaction, leading to an increased steady-state ATPase rate. In any case, the low basal and high microtubule-activated ATPase rates of K339 in solution further corroborate the notion that the N-terminal 339 aa of KHC represent a relatively stable, independently folded mechanochemical domain.

ncd Protein Minimal Motor Domain. The ncd protein is predicted to have an extended α-helical, coiled-coil domain that separates the C-terminal motor domain from a potentially globular N-terminal tail domain (Fig. 1*B*). The predicted coiled-coil region extends up to aa 320, which is the approximate beginning of sequence similarity with the conserved region of the kinesin superfamily (7, 8). By analogy to the experiments with KHC, a series of ncd truncations was created to determine whether the domain structure of the ncd protein was essential for microtubule motor activity or direction of microtubule movement. Removal of the tail domain (GST-N195) had little effect on the rate or direction of microtubule movement by the ncd protein. Increasing truncation of the ncd protein (GST-N280 and GST-N300) resulted in declining rates of microtubule motility. Complete removal of the coiled-coil region (GST-N320) caused an ≈100-fold decrease in motility rate. The (−)-end-directed microtubule motility by GST-N320 (Fig. 2 *d–f*) demonstrates that the conserved domain of the ncd protein is intrinsically (−)-end-directed, and therefore, the organization and sequences of the nonconserved domains do not contribute to the direction of microtubule movement by the ncd protein.

Since the effects of truncation on the rates of ncd motility were similar to the truncation effects on KHC motility, we compared the steady-state ATPase activities of GST-N195 and GST-N320 in solution to determine whether, by analogy to GST-K339, the ATPase activity of GST-N320 was dramatically elevated. From double reciprocal plots of ATP hydrolysis rate versus microtubule concentration, V_{max} and the microtubule K_m for GST-N195 were 0.3 s^{-1} and 2.3 μM. For GST-N320, V_{max} and the microtubule K_m were 0.6 s^{-1} and 6.0 μM. ATP hydrolysis rates in the absence of microtubules for GST-N195 and GST-N320 were 0.02 s^{-1} and 0.03 s^{-1}, respectively. In contrast to GST-K339, the microtubule-activated ATPase rate of GST-N320, relative to GST-N195, is apparently not elevated dramatically. However, the percent of active protein in the preparations, which was not estimated, could be significantly different and mask an elevated rate. In any case, the nearly 100-fold decline in motility rate is not accompanied by a 100-fold decline in enzymatic activity. It is interesting that V_{max} of the ncd proteins is substantially lower than V_{max} of the KHC proteins because of much less activation by microtubules. Similar to the argument for GST-K339, the ATPase activity of GST-N320 suggests that the conserved domain of the ncd protein is a relatively stable and independent motor domain.

In summary, our results demonstrate that the conserved regions of both KHC and ncd are sufficient for force generation and microtubule motor activity. Further, the direction of movement is intrinsic to both the KHC and the ncd protein motor domains, which narrows the search for the determinants of direction to ≈340 aa. Finally, while the nonconserved portions of kinesin-like proteins are likely to modulate and fine tune the activities of the kinesin superfamily motor domain, the observations presented here lend strong support to the concept that the conserved domain of the kinesin superfamily is an independent and adaptable mechanochemical domain.

We thank Mr. David Woerpel for putting together the pGEX-K360 plasmid. This work was supported by an American Cancer Society faculty research award and a National Institutes of Health grant (L.S.B.G.) and a National Institutes of Health postdoctoral fellowship (R.J.S.).

1. Endow, S. A. (1991) *Trends Biochem.* **16,** 221–225.
2. Goldstein, L. S. B. (1991) *Trends Cell Biol.* **1,** 93–98.
3. Yang, J. T., Laymon, R. A. & Goldstein, L. S. B. (1989) *Cell* **56,** 879–889.
4. Yang, J. T., Saxton, W. M., Stewart, R. J., Raff, E. C. & Goldstein, L. S. B. (1990) *Science* **249,** 42–47.
5. Walker, R. A., Salmon, E. D. & Endow, S. A. (1990) *Nature (London)* **347,** 780–782.
6. McDonald, H. M., Stewart, R. J. & Goldstein, L. S. B. (1990) *Cell* **63,** 1159–1165.
7. Endow, S. A., Henikoff, S. & Soler-Neidziela, L. (1990) *Nature (London)* **345,** 81–83.
8. McDonald, H. M. & Goldstein, L. S. B. (1990) *Cell* **61,** 991–1000.
9. Dubreuil, R. R., Byers, T. J., Sillman, A. L., Bar-Zvi, D., Goldstein, L. S. B. & Branton, D. (1989) *J. Cell Biol.* **109,** 2197–2205.
10. Smith, D. B. & Johnson, K. S. (1988) *Gene* **67,** 31–40.
11. Guan, K. L. & Dixon, J. E. (1991) *Anal. Biochem.* **192,** 262–267.
12. Harada, Y., Sakurada, K., Aoki, T., Thomas, D. D. & Yanagida, T. (1990) *J. Mol. Biol.* **216,** 49–68.
13. Hyman, A. A. (1991) *J. Cell Sci. Suppl.* **14,** 125–127.
14. Kodama, T., Fukui, K. & Kometani, K. (1986) *J. Biochem. (Tokyo)* **99,** 1465–1472.
15. Lupas, A., Dyke, M. V. & Stock, J. (1991) *Science* **252,** 1162–1164.
16. Kosick, K. S., Orecchio, L. D., Schnapp, B., Inouye, H. & Neve, R. L. (1990) *J. Biol. Chem.* **265,** 3278–3283.
17. Kuznetsov, S. A., Vaisberg, Y. A., Rothwell, S. W., Murphy, D. B. & Gelfand, V. I. (1989) *J. Biol. Chem.* **264,** 589–595.
18. Ingold, A. L., Cohn, S. A. & Scholey, J. M. (1988) *J. Cell Biol.* **107,** 2657–2667.